



UNIVERSITY OF LEEDS

This is a repository copy of *Groundwater flow velocities in karst aquifers; importance of spatial observation scale and hydraulic testing for contaminant transport prediction*.

White Rose Research Online URL for this paper:

<https://eprints.whiterose.ac.uk/176356/>

Version: Accepted Version

---

**Article:**

Medici, G and West, LJ [orcid.org/0000-0002-3441-0433](https://orcid.org/0000-0002-3441-0433) (2021) Groundwater flow velocities in karst aquifers; importance of spatial observation scale and hydraulic testing for contaminant transport prediction. *Environmental Science and Pollution Research*, 28 (32). pp. 43050-43063. ISSN 0944-1344

<https://doi.org/10.1007/s11356-021-14840-3>

---

© Crown 2021. This is an author produced version of an article, published in *Environmental Science and Pollution Research*. Uploaded in accordance with the publisher's self-archiving policy.

**Reuse**

Items deposited in White Rose Research Online are protected by copyright, with all rights reserved unless indicated otherwise. They may be downloaded and/or printed for private study, or other acts as permitted by national copyright laws. The publisher or other rights holders may allow further reproduction and re-use of the full text version. This is indicated by the licence information on the White Rose Research Online record for the item.

**Takedown**

If you consider content in White Rose Research Online to be in breach of UK law, please notify us by emailing [eprints@whiterose.ac.uk](mailto:eprints@whiterose.ac.uk) including the URL of the record and the reason for the withdrawal request.



[eprints@whiterose.ac.uk](mailto:eprints@whiterose.ac.uk)  
<https://eprints.whiterose.ac.uk/>

1 **Groundwater flow velocities in karst aquifers; importance of spatial observation scale and hydraulic testing**  
2 **for contaminant transport prediction**

3

4 Giacomo Medici<sup>1\*</sup>, Landis Jared West<sup>2</sup>

5 <sup>1</sup> G<sup>360</sup> Institute of Groundwater Research, University of Guelph, Stone Road, Guelph, Ontario, N1G 2W1, Canada

6 <sup>2</sup> School of Earth and Environment, University of Leeds, Woodhouse Lane, Leeds, W Yorkshire LS2 9JT, UK

7 \* Corresponding author: giacomo.medici@g360group.org

8

9 **Abstract**

10 We review scale dependence of hydraulic conductivities and effective porosities for prediction of contaminant  
11 transport in four UK karst aquifers. Approaches for obtaining hydraulic parameters include core plug, slug, pumping  
12 and pulse tests, calibration of groundwater flow models, and spring recession curves. Core-plug and slug tests are  
13 unsuitable because they do not characterise a large enough volume to include a representative fracture network.  
14 Pumping test values match regional-scale hydraulic conductivities from flow modelling for the less intensively  
15 karstified aquifers: Magnesian Limestone, Jurassic Limestone and Cretaceous Chalks. Reliable bulk hydraulic  
16 conductivities were not available for the intensively-karstified Carboniferous Limestone due to dominance of flow  
17 through pipe-conduits in the Mendips. Here, the only hydraulic conductivity value found from springs recession is  
18 one order of magnitude higher than that indicated by pumping tests. For all four carbonate aquifers, effective  
19 porosities assumed for transport modelling are two orders of magnitude higher than those found from tracer and  
20 hydrogeophysical tests. A combination of low hydraulic conductivities and assumed flowing porosities, has resulted  
21 in underestimated flow velocities. The UK karst aquifers are characterized by a range of hydraulic behaviours that  
22 fit those of karst aquifers worldwide. Indeed, underestimation of flow velocity due to inappropriate parameter  
23 selection is common to intensively karstified aquifers of southern France, north-western Germany and Italy. Similar  
24 issues arise for the Canadian Silurian carbonates where high effective porosities (e.g., 5%) used in transport models

25 leads to underestimation of groundwater velocities. We recommend values in the range of 1% - 0.01% for such  
26 aquifers.

27 **Keywords** Karst; Flow velocity; Effective porosity; Hydraulic conductivity; Tracer tests; Hydro-geophysics

28

## 29 **Introduction**

30 Carbonate aquifers, which are subjected to different degrees of karstification underlie a land area covering ~15% of  
31 the earth surface and supply ~25% of the world population with drinking water (see Fig. 1; Goldscheider et al.  
32 2020). However, at the scale of Great Britain (Fig. 2), karst aquifers of carbonate origin supply with 55% of  
33 groundwater production. This proportion is distributed as follows amongst the four major karst aquifers of United  
34 Kingdom; both Northern and Southern Chalks (~35%), Jurassic Limestone (10%), Carboniferous Limestone (6%)  
35 and Magnesian Limestone (4%) (Allen et al. 1997; MacDonald and Allen 2001; Rivett et al. 2007; Abesser and  
36 Lewis 2015). These aquifers of marine carbonate origin represent the focus of this review, but their hydraulic  
37 properties are analogous to other European and North American aquifers. A range of pollutants can reach the  
38 saturated part of karst aquifers in all the regions which are devolved to industry and agriculture across the world.  
39 These contaminants include nitrate, sulphate, chloride, toxic organic compounds released by mineral fertilizers and  
40 pesticides, and pathogens (Tratner et al. 1997; Drew 2008; Reimann and Hill 2009; Göppert and Goldscheider 2011;  
41 Gregory et al. 2014; Reh et al. 2014; Palmucci et al. 2016; Liu et al. 2019; Medici et al. 2019c, 2020; Rusi et al.  
42 2018; Ducci et al. 2019; Parker et al. 2019; Ren et al. 2019). Fast transport of such pollutants typically occurs  
43 through bedding plane discontinuities, joints, and fault-related fractures rather than via porous matrix in lithified  
44 carbonate rocks (Berkowitz 2002; West and Odling 2007; Medici et al. 2016, Jones et al. 2017; Maldaner et al.  
45 2018; Berlin et al. 2020; Hu et al. 2020). This category of fractured aquifers is particularly prone to solutional  
46 widening of rock discontinuities and are hence the most vulnerable because contaminant plumes are transported at  
47 relatively high rates.

48 A significant increase of modelling-oriented literature has been produced in karst hydrogeology in the last 15 years  
49 reflecting the high vulnerability of carbonate aquifers (e.g., Reimann and Hill 2009; Hill et al. 2010; Gallegos et al.  
50 2013; Saller et al. 2013; Assari et al. 2017; Sullivan et al. 2019). These recent advances in modelling fluid flow in  
51 the subsurface are frequently not accompanied by a corresponding increase in the use of hydraulic testing. As a  
52 consequence, modelling might not capture the complexity of these systems, which require parameters such as

53 hydraulic conductivity and effective porosity that can vary with scale (Le Borgne et al. 2006; Amoruso et al. 2013;  
54 Medici et al. 2020).

55 From a conceptual point of view using the Equivalent Porous Medium (EPM) approach, the groundwater flow  
56 velocity ( $V$ ) is controlled by three factors, which are hydraulic gradient ( $i$ ), hydraulic conductivity ( $K$ ) and effective  
57 flow porosity ( $\Phi_e$ ) according to the Equation (1),

58

$$59 \quad V = -\frac{Ki}{\Phi_e} \quad (1)$$

60

61 Numerical simulations usually rely on measured hydraulic heads in wells for calibration with respect to hydraulic  
62 gradient. However, it is more challenging to define  $K$  and  $\Phi_e$ . Indeed, EPM is commonly used to model groundwater  
63 flow and contaminant transport in relatively large ( $\sim 10^2 - 10^3 \text{ km}^2$ ) areas, although much smaller scale discrete  
64 conduits characterized by turbulent flow can be inserted if the network is known by geophysical and speleological  
65 surveys (Hill et al. 2010; Saller et al. 2013; Chen and Goldscheider 2014; Hartmann et al. 2014).

66 Hydraulic conductivity is commonly poorly defined at the scale of groundwater flow and transport models of karst  
67 aquifers, which can cover areas of tens of kilometres (Anderson and Cherry 1979; Gleeson et al. 2011). Typically,  
68 the hydraulic conductivity rises moving from the scale of core plug to the one of slug and packer tests, which sample  
69 rock matrix and fractures, respectively. Hydraulic conductivity is typically one order of magnitude higher still,  
70 where testing larger volumes of the aquifer with long duration pumping tests, because these include more permeable  
71 features such as conduit networks (Hartmann et al. 2014; Ren et al. 2018; Medici et al. 2019a, b). Many numerical  
72 simulations rely on the concept of Representative Elementary Volume (REV) in order to define appropriate values  
73 for the hydrogeological properties. According to the latter concept, above a threshold volume known as the REV,  
74 properties become invariant with scale. In the case of karst aquifers, due to the spatial properties of karst networks,  
75 REVs may be relatively large (i.e. site scale or above) or indeed no effective REV may exist as properties continue  
76 to change with scale up to the volume of an entire catchment (Kiralý 1975).

77 Given its scale dependence, determination of aquifer hydraulic conductivity by numerical model calibration, but  
78 constrained by field test values is arguably the best approach. However, a calibration approach remains subject to  
79 uncertainty due to difficulties in defining the other parameters (e.g. rainfall recharge) that are part of the  
80 parameterized inversion. Even more challenging is defining appropriate effective porosity for particle tracking and

81 solute transport models. In fact, this hydraulic parameter is usually not subject to any calibration process.  
82 Approaches for field determination of effective porosity ( $\Phi_e$ ) include combining tracer and pumping tests to provide  
83 the flow velocity ( $V$ ) and hydraulic conductivity ( $K$ ), respectively (see Equation 1; Worthington et al. 2012;  
84 Worthington 2015). The effective porosity can also be calculated using borehole hydro-geophysics by applying the  
85 cubic law either coupling fluid logging and slug tests (Ren et al. 2018; Medici et al. 2019a), combining borehole  
86 dilution (tracer) and packer tests (Maldaner et al. 2018) or using borehole dilution response to distribute well  
87 transmissivity to specific intervals or features (Agbotui et al. 2020). The use of these recent published approaches to  
88 determine effective porosity is not standard practice in hydrogeology as such tests are typically not conducted prior  
89 to numerical simulations. Hence, the risk of computing unreliable groundwater flow velocities is significant for  
90 fractured carbonates (Brunetti et al. 2013; Worthington 2015). Note that, determination of groundwater flow  
91 velocities finds practical application in the design of capture zone around springs and abstraction wells. The spatial  
92 definition of capture zones is intended to protect drinkable water from contamination and thereby preserve public  
93 health in karst environments (Medici et al. 2019b).

94 In this review, we highlight how underestimation of groundwater flow velocities by more than one order of  
95 magnitude arise from either paucity or lack of hydraulic tests, with reference to the principal karst aquifers of Great  
96 Britain. We show in detail how the combination of difficulties in defining aquifer hydraulic conductivity and  
97 effective porosity lead to possible large underestimation of flow velocities in these and similar aquifers of Europe  
98 and North America. Our purpose is to direct groundwater flow modellers towards a rigorous practice that avoids  
99 underestimation of flow velocities and hence unrealistic and spatially reduced capture zones around abstraction  
100 areas. Our workflow involves: (i) comparison of effective porosity values extracted at different scales from hydro-  
101 geophysical and tracer testing in the four major UK aquifers, (ii) reviewing data on scale dependence of hydraulic  
102 conductivity in these carbonate aquifers, and (iii) identification of specific examples of underestimation of flow  
103 velocities in EPM models, where such underestimation arises from paucity of hydraulic testing data.

104

### 105 **Karst in Great Britain**

106 The Cretaceous Chalk (Fig. 3a), the Jurassic Limestone (North Province shown in Figure 3b), the Magnesian  
107 Limestone (Fig. 3c, d), and the Carboniferous Limestone (Fig. 3e) aquifers have different depositional histories  
108 (Hallam 1971; Chadwick et al. 1993). The Carboniferous Limestone is related to deep carbonate sedimentation and

109 sandstone and shaly beds also occur in the sedimentary sequence. The Chalk is related to deep marine sedimentation  
110 with deposition of carbonate ooze during the Cretaceous in Great Britain (Hancock 1975; Jeans 1980; Alexander et  
111 al. 2012). Here, the Cretaceous Chalk is differentiated in a Northern and Southern Province based on the degree of  
112 induration (Allen et al. 1997; Aliyu et al. 2017). The Magnesian Limestone is related to shallow water deposition at  
113 the margins of the Zechstein basin during the Permian (Tucker 1991; Mawson and Tucker 2009). The Jurassic  
114 Limestone is related to both shallow and deep marine carbonate sedimentation that occurred during the  
115 fragmentation of the Tethys Ocean (Wignall and Newton 2001). Despite differences in their depositional history the  
116 four major UK aquifers are all characterized by relatively non-conductive ( $10^{-6}$ - $10^{-1}$  m/day) matrix but allow rapid  
117 transport of water and pollutants via fractures, fissures (solutionally widened fractures) and conduits (Fig. 3; Allen et  
118 al. 1997).

119 Important groundwater resources are stored in karst aquifers in the United Kingdom and hence a large amount of  
120 hydraulic data have been collected (e.g., Allen et al. 1997). Distribution of aquifer permeability from pumping test  
121 data presented as transmissivity vs. cumulative frequency plots (Fig. 4.; Worthington and Ford 2009) individuate the  
122 Carboniferous Limestone and the Cretaceous Chalk as end members in terms of extent of karstification (Atkinson  
123 and Smart 1981; Worthington and Ford 2009). Indeed, the Carboniferous Limestone (Fig. 3d) is characterized by  
124 sinking streams, large number of sinkholes and dolines, caves and much discharge through channels (Hobbs and  
125 Gunn 1998; Farrant and Cooper 2008; Worthington and Ford 2009; Kana et al. 2013). The other end member is the  
126 Chalk, has fewer, smaller conduits, with Darcian flow along bedding plane fractures, joints and faults being  
127 dominant in most areas, although more substantive conduit development occurs when sinking streams occur near the  
128 edge of overlying less permeable formations (Fig. 3a; Bloomfield 1996; Maurice et al. 2006; Worthington and Ford  
129 2009; Odling et al. 2013; Sorensen et al. 2013). The Jurassic Limestone and Magnesian Limestone are considered  
130 intermediate aquifer types with distribution of pumping test data closer to the curve of the Cretaceous Chalk than the  
131 Carboniferous Limestone (see Fig. 4). This analysis of the UK karst aquifers by Worthington and Ford (2009)  
132 represents the starting point of our review that extends their analysis via integration of data from core plug, slug and  
133 pumping tests, recession of springs, tracer tests and hydro-geophysics from a number of authors as summarized  
134 below.

135

136

### 137 *Hydraulic Conductivity*

138 Establishing representative hydraulic conductivity values to use in particle tracking and solute transport models is  
139 difficult due to the scale dependence of this parameter in karst systems. In fact, hydraulic tests such as slug tests and  
140 long duration pumping tests sample aquifer hydraulic conductivity with  $\sim 10^{-1}$ - $10^0$  and  $\sim 10^1$ - $10^2$  m length scales,  
141 respectively (Figs. 5 and 6). For example, the use of single-borehole pumping tests that are characterized by a  
142 unique well with a pumping radius of influence of 50-150 m is the most common approach for characterization of  
143 hydraulic conductivity in the karst aquifers analysed here (Allen et al. 1997). In contrast, groundwater flow, particle  
144 tracking, and solute transport models sample hydraulic parameters over much larger areas. Particle tracking to  
145 abstraction wells, springs and streams typically cover flowpath distances in the range of  $\sim 10$ - $100$  km (Medici et al.  
146 2019b). Hence, problems of spatial representation can arise.

147 The Cretaceous Chalk, which represents the principal UK aquifer in terms of abstraction volumes and hosts  
148 important hydrocarbon resources in the North Sea, has received most attention in terms of research efforts over the  
149 years (Allen et al. 1997; Wang et al. 2012; Aliyu et al. 2017; Souque et al. 2019). Thus, complete sets of hydraulic  
150 data from the core plug to the regional scale of groundwater flow and transport models are available for the Northern  
151 Province Chalk in in NE Yorkshire as well as the Southern Province Chalk in Hertfordshire (Area 1 and Area 2 in  
152 Figure 2). Data from the other three karst aquifers is available mainly from groundwater hydraulic testing and  
153 MODFLOW model calibration (e.g. Areas 3, 4, 5 in Fig. 2, Allen et al., 1997). Hydraulic conductivity sharply rises  
154 with increasing the observation scale moving from core plug, to slug test and up to pumping test scale for all four  
155 aquifers (Cretaceous Chalk, Jurassic Limestone, Magnesian Limestone and Carboniferous Limestone respectively,  
156 see Figures 5 and 6). Notably, for Cretaceous Chalk the hydraulic conductivity at the regional scale, obtained from  
157 MODFLOW model calibration, matches the interquartile range of pumping tests for both Northern and Southern  
158 Province Chalks (see Fig. 5a and b respectively). This scenario is typical of non-intensively karstified aquifers that  
159 behave as quasi-homogeneous systems at the regional scale and the upper bound in terms of hydraulic conductivity  
160 is given by pumping tests (Schulze-Makuch et al. 1999). The Chalk presents a range of hydraulic conductivity (Fig.  
161 5) values due to the fact that the aquifer is more conductive in dry valleys and streams (Maurice et al. 2006; Odling  
162 et al. 2013). Here, groundwater flow modellers have typically assigned higher values of hydraulic conductivity in  
163 the position of valleys and streams in both Northern Province (Fig. 5a) and Southern Province (Fig. 5b) Chalks.

164 The scenario in terms of variation of hydraulic conductivity with the spatial scale increase observed in the Chalk  
165 (see Fig. 5a, b) is similar to those for the Jurassic (Fig. 6a) and the Magnesian Limestone (Fig. 6b) aquifers (see Fig.  
166 2 for locations), i.e., hydraulic conductivity rises from the scale of core plugs, to slug tests and pumping tests. The  
167 upper bound in terms of hydraulic conductivity from MODFLOW model calibration is also captured at the scale of  
168 the well-tests in the Jurassic and the Magnesian Limestone aquifers, i.e. the regional-scale hydraulic conductivity  
169 from MODFLOW groundwater flow models falls largely within the interquartile ranges of hydraulic conductivity  
170 from pumping tests. Slug tests provide lower mean values than pumping tests and are hence unreliable indicators of  
171 hydraulic conductivity in these karst aquifers (Figs. 5, 6a, b).

172 Overall, the Chalk, the Magnesian and the Jurassic Limestone aquifers of Great Britain show a similar pattern of  
173 variation in terms of hydraulic conductivity. This hydraulic scenario matches the cumulative frequency plots of  
174 transmissivities from pumping tests proposed by Worthington and Ford (2009) that show partial superimposition of  
175 the curves (Fig. 4). Notably, these non-intensively karstified aquifers show a match between pumping tests and  
176 groundwater flow model-derived hydraulic conductivity (Figs. 5, 6a, b).

177 Similarly to the other three aquifers, the Carboniferous Limestone (Figs. 2, 6c) in the Mendips of southern England  
178 is characterized by increasing hydraulic conductivity from the core plug up to the scale of pumping tests. However,  
179 the regional scale hydraulic conductivity computed by Atkinson (1977) by analysing recession of springs is 89  
180 m/day; more than one order of magnitude higher than the median of pumping test values (Fig. 6c). This scenario  
181 matches the cumulative frequency curve of transmissivity shown in Figure 4 that depicts the Carboniferous  
182 Limestone as an end member with regards to karstogenesis (Atkinson 1977; Worthington and Ford 2009). Here,  
183 groundwater flow is dominated or exclusively occurs in pipe conduits of several m of diameter (Fig. 3e), which are  
184 characterized by turbulent flow.

185 Groundwater flow in these karstic features should ideally be represented by a conductance term instead of a  
186 hydraulic conductivity (Shoemaker et al. 2008; Hills et al. 2010; Chen and Goldscheider et al. 2014). The  
187 conductance is defined as the ratio between the volumetric flow rate through a pipe and the hydraulic gradient  
188 (Shepley et al. 2012; Medici et al. 2021b). Thus, the hydraulic conductivity defined by spring recession (Atkinson  
189 1977) will be non-unique and depend on the hydraulic gradient, which may explain differences in pumping tests  
190 (Gallegos et al. 2013; Saller et al. 2013). Details on the use of a network of discrete conduits vs. Equivalent Porous  
191 Medium approach in carbonate aquifers were investigated in a previous USGS manual (Shoemaker et al. 2008) and

192 are discussed by Hartman et al. (2014). However, numerical models that represent turbulent flow in pipe conduits of  
193 karstic origin have not been developed yet in the UK Carboniferous Limestone, which is still modelled using EPM  
194 for regional groundwater flow modelling (Shepley et al. 2012).

195

### 196 *Effective Porosity*

197 Groundwater flow velocities are increased as the effective porosity reduces, provided that both hydraulic  
198 conductivity (K) and hydraulic gradient (i) remain constant, according to Equation 1. In fractured and karstic aquifer  
199 systems, effective porosity is often relatively small because both fracture networks and conduits represent a low  
200 proportion of the rock volume. Thus, choosing unrepresentative large values for effective porosity leads to  
201 underestimated transport velocities of contaminants in the subsurface. Values of effective porosity of between 1%  
202 and 10% have previously been recommended to use in solute transport and particle tracking models in karst aquifers  
203 (Freeze and Cherry 1979). Notably, where hydro-geophysical and tracer tests data are available, values measured in  
204 the four carbonate aquifers of Great Britain are much smaller than this ‘applied standard’ value and range, typically  
205 between 0.01% and 1% (Fig. 7). For example, average effective porosities of 0.01% and 0.21% were computed in  
206 the Chalk using tracer tests and well dilution tests, respectively (Fig. 7; Cook et al. 2012; Agbotui et al. 2020). These  
207 effective porosities for the Cretaceous Chalk are much smaller than the core-plug values of total porosity from the  
208 matrix blocks (22-38% of interquartile range; Allen et al. 1997), probably because small pore throat sizes ranging  
209 from 0.2 and 1 microns restrict advective flow into the matrix. The experimental results for effective porosity at the  
210 scale of single-well dilution and well-to-well tracer tests contrast strongly with the value of 1% used to run solute  
211 contaminant transport in the Chalk of Hertfordshire and Cambridgeshire (Little et al. 1986; Allen et al. 1997;  
212 Worthington 2015 ). Such a high value of effective porosity has been previously justified to account for the ability  
213 of solutes to enter the matrix porous blocks via diffusion. However, these high values (~1%) of effective porosity  
214 are not appropriate in particle tracking models used to define well-head protection zones around abstraction wells,  
215 where the inner and outer well-head protection zones are typically defined to protect abstraction wells from viruses  
216 and bacteria. These organisms are too large to enter small pores and diffuse in the matrix (Taylor et al. 2004;  
217 Environment Agency 2019).

218 Hydraulic scenarios are also illustrated in Figure 7 for the Jurassic Limestone and the Magnesian Limestone  
219 aquifers, i.e. modellers are using much higher effective porosity values than those from hydro-geophysical and

220 tracer testing, by up to two order of magnitude. Values of average effective porosity of 0.01% and 0.03% were  
221 computed using tracer tests and by combining slug tests and fluid logging in the Jurassic Limestone and the  
222 Magnesian Limestone, respectively (Foley et al. 2012; Medici 2019a, b), whereas values used to simulate  
223 contaminant transport in both aquifers were ranged from 1% to 10% (Fig. 7).

224 Overall, the scenario illustrated in Figure 7 indicates an overestimation of up to two orders of magnitude in flowing  
225 porosity ( $\Phi_e$ ) and hence an underestimation (see Equation 1 assuming constant K and i) in the groundwater flow  
226 velocities in the studied carbonate aquifers. This large underestimation in groundwater flow velocities is supported  
227 both by borehole hydro-geophysical and well-to-well tracer testing and results in incorrectly small protection zones  
228 around abstraction wells (Worthington 2015). Source protection for three wells in the Jurassic Limestone near  
229 Scarborough, Yorkshire, UK were modelled with MODFLOW-MODPATH, giving a 50 day-time of travel zones  
230 that extended up to 1.6 km upgradient from the wells. However, subsequent tracer testing from a losing stream reach  
231 showed that tracers travelled 7 km to the wells in only 3-11 days (Foley et al. 2012). Such travel times support an  
232 effective porosity value of  $\sim 0.01\%$  to match the modelled capture zone with tracer testing data (Worthington 2015).  
233 Hence, such a low effective porosity value is supported at both the scale of borehole hydro-geophysical tests ( $\sim 10^1$ -  
234  $10^2$  m) as well as of point-to-point tracer testing ( $\sim 10^3$ - $10^4$  m) that includes typical spatial extent of capture zones  
235 around abstraction wells (Worthington 2015; Medici et al. 2019b).

236 Notably, values of effective porosity from particle tracking models are absent for the Carboniferous Limestone of  
237 England, as no such models have been developed. Indeed, approaches for the Carboniferous Limestone aquifer have  
238 instead been via characterization of discrete conduits and fissures (the effective flowing structures) by tracer tests  
239 and geo-radar surveys for definition of flow velocities and spatial dimension, respectively (Hobbs 1988; Allen et al.  
240 1997; Pringle et al. 2002; Kana et al. 2013). Tracer tests indicate flow velocities up to 21 km/day, the highest among  
241 the four UK karst aquifers, in the large cavities of the Carboniferous Limestone aquifer in the Mendips (see Fig. 2).  
242 As a result, large capture zones were delineated (Allen et al. 1997).

243

#### 244 **UK karst aquifers vs. analogous successions**

245 Groundwater flow, particle tracking, and solute transport models typically cover areas of  $\sim 10^4$ - $10^{10}$  m<sup>2</sup> (Davison and  
246 Lerner 2000; Neymeyer et al. 2007) whereas those sampled by pumping tests are towards the lower end of this range  
247 (areas of  $\sim 10^4$ - $10^5$  m<sup>2</sup>). Notably, spatial misfit between the hydraulic test- and model-scale typically arises in

248 numerical models of chemical industrial sites and large administrative areas such as counties and states, which are  
249 typically developed by national or state Geological Surveys or regulatory bodies (e.g., Ely et al. 2015). Hydraulic  
250 conductivity at the model scale in all these cases can be higher than those measured by both slug and pumping tests  
251 as postulated by Kiraly (1975) for the intensively karstified aquifers of France. The scale dependence of hydraulic  
252 conductivity typically arises because the number of hydraulic connections rises progressively with scale including a  
253 larger aquifer volume and hence different types of rock discontinuities. In fact, large bedding plane discontinuities  
254 related to angular unconformities, joints and faults often lead to a high degree of hydraulic connectivity at  
255 observation scales larger than those shown by both slug and pumping tests (Berkowitz 2002; White 2002; Hartmann  
256 et al. 2014).

257 Manuals of groundwater flow modelling recommend to slightly modify values of slug and pumping tests in the  
258 model calibration process using these values as lower and upper boundaries in the Tikhonov regularization in the  
259 PEST package (Doherty and Hunt 2016). However, we suggest to discard values of hydraulic conductivity from slug  
260 tests, prior to using these results to set limits for calibration of groundwater flow models in karst aquifers (see plots  
261 in Figures 5 to 6c). The lower values of hydraulic conductivity from pumping tests can be used as limits. By  
262 contrast, the highest values of pumping tests cannot represent a boundary in a calibration process due to  
263 uncertainties in the REV from the scale of industrial site and up to the regional scale.

264 Hydraulic conductivity in the highly karstified carbonate aquifer of the Carboniferous Limestone is characterized by  
265 a regional scale hydraulic conductivity higher than the maximum value from pumping tests (Fig. 6c). Similar  
266 hydraulic scenarios can also be found in carbonate aquifers overseas. Indeed, a groundwater flow model of the  
267 travertine of central Italy found calibrated values of hydraulic conductivities higher than those from pumping tests  
268 by one order of magnitude. This modelling result arises from the presence of a highly karstified normal fault of  
269 Quaternary age that was not sampled by pumping tests (Brunetti et al. 2013). An increase in hydraulic conductivity  
270 of one up to two order of magnitude was also found in the highly karstified limestone of south-western Germany  
271 moving up from the scale of the pumping test to the regional scale (Sauter 1992; Schulze-Makuch et al. 1999).

272 Noushabadi et al. (2011) demonstrated how in the Mesozoic fractured and karst aquifers of southern France,  
273 hydraulic conductivity rises by up to two order of magnitude moving from the scale of pumping tests to those of  
274 pulse tests. The latter type of well tests allow testing aquifer areas of up to 40 km in length by sending a coded  
275 hydraulic signal from a producing well to a shut-in observation well (Johnson et al. 1966). Note that, such high

276 hydraulic conductivities measured by pulse tests were related to karstification, which enlarge connective rock  
277 discontinuities.

278 Findings from the highly karstified aquifers of south England (Atkinson 1977), south-western Germany (Sauter  
279 1992), central Italy (Brunetti et al. 2013) and southern France (Noussabadi et al. 2011) highlight the discrepancy  
280 between the hydraulic conductivity from slug and pumping tests and those required to accurately predict transport  
281 velocities of pollutants. To sum up, we propose an approach to calibration of regional groundwater flow models that  
282 discard values of slug tests, and do not use the highest values of pumping tests as upper limit in favour of those of  
283 pulse tests should those be available.

284 However, more widespread international underestimation of groundwater flow velocities of two orders of magnitude  
285 appears also possible from mis-estimation of values of effective porosity. Frequently a value of ~1% for flow  
286 porosities in carbonate rocks are typically adopted to model particle tracking and solute transport using MODPATH  
287 and MT3DMS, respectively. Indeed, a 5% effective porosity has been recently used for the studied Permian  
288 dolostone of NE England (Neymeyer et al. 2007), Cambrian-Ordovician limestone of Nevada (Bredehoeft and King  
289 2010), the Silurian Dolostone of Ontario (Golder Associates, 2006), the Jurassic limestone of southern Italy  
290 (Zuffianò et al. 2016) and the Cretaceous dolostone of southern Spain (Gárfias et al. 2018). These workers do not  
291 support their values of effective porosity by citing tracer tests or borehole hydro-geophysical data, their 5% value is  
292 likely simply assigned as standard for fractured aquifers, based on previous practice.

293 By contrast, extrapolation of effective porosities by applying the cubic law combining slug tests with fluid or well  
294 dilution tests reveals much lower values (0.02% – 0.04%) in the Permian dolostone of NE England, the Silurian  
295 dolostone of Ontario and the other karst aquifers listed in Fig. 6c. In addition of the above mentioned methods,  
296 values of effective porosity were more recently investigated in the Silurian Dolostone of Ontario by applying the  
297 cubic law using FLUTE and Straddle Packer testing that provide average values of 0.06% and 0.03%, respectively  
298 (Munn 2012; Trudell 2014). Well-to-well tracer tests investigate the rock volume at a larger scale (with respect to  
299 the above mentioned methods) also indicate a low value (0.05%) of effective porosity for the Silurian Dolostone of  
300 Ontario (Worthington et al. 2012). Thus, lack of aquifer hydraulic testing appears a further cause of underestimation  
301 of groundwater flow velocities via errors in the assumed values for effective porosity as well as hydraulic  
302 conductivity.

303 Caution is needed to apply our review in some specific case studies, evidence is shown that enlargement of fractures  
304 by groundwater leaching can increase the effective porosity in karst aquifers up towards values ~1%. Matches  
305 between groundwater ages and average travel times computed using MODPATH in the Palaeozoic Limestone of  
306 Virginia were achieved by using 1% as effective porosity to characterize the Equivalent Porous Medium. However,  
307 in these cases hydraulic conductivity (at the scale higher than those of pumping tests) is likely also subject to an  
308 increase, as demonstrated in the highly karstified limestones of southern France and Italy and south-western  
309 Germany (Saler 1992; Brunetti et al. 2013; Noushabadi et al. 2011), which will again lead to very high groundwater  
310 velocities. Indeed, in these studies, pumping tests show values lower than the regional-scale hydraulic conductivity.  
311 Paucity of hydraulic testing and application of ‘standard values’ of effective porosity in groundwater flow models  
312 would lead even in the latter cases to an underestimation of groundwater flow velocities in karst aquifers. Hence,  
313 capture zones around abstraction wells and springs tend to be larger in carbonate aquifers with respect to those sited  
314 on crystalline and other sedimentary rocks (Perrin et al. 2011; Le Borgne et al. 2011; Medici et al. 2019b; Parker et  
315 al. 2019).

316

### 317 **Conclusions**

318 Groundwater flow velocities are controlled by three factors, which are hydraulic gradient, hydraulic conductivity  
319 and effective porosity. Numerical models usually rely on measured hydraulic heads in wells to estimate the  
320 hydraulic gradient. More problematic is the definition of effective porosity and hydraulic conductivity in karst  
321 aquifers at the appropriate scale of investigation that is needed for particle tracking and solute transport models. To  
322 address this issue, the hydraulic properties of the major carbonate aquifers of Great Britain, the Carboniferous  
323 Limestone, Magnesian Limestone, Jurassic Limestone and Northern and Southern Province Cretaceous Chalks, were  
324 reviewed from the scale of the core plug tests, small scale hydraulic tests such as slug tests, larger scale pumping  
325 tests and regional scale estimates from model calibration. This analysis shows how paucity of hydraulic testing has  
326 historically led to underestimation of appropriate values for hydraulic conductivity and overestimation of effective  
327 porosity, respectively, at groundwater and solute transport modelling scales. We show that the systematic  
328 underestimation of groundwater flow velocities has been the norm for these systems.

329 The intensively karstified Carboniferous Limestone shows a regional-scale hydraulic conductivity that is higher by  
330 one order of magnitude with respect to that indicated by the pumping tests, leading to underestimation of

331 groundwater velocities. Although there is better agreement between pumping test and regional-scale hydraulic  
332 conductivity in the more moderately karstified aquifers (Magnesian Limestone, Jurassic Limestone and Northern  
333 and Southern Cretaceous Chalk aquifers), in all four cases, effective porosities typically used to run particle tracking  
334 and solute transport models are two order of magnitude higher than those measured by tracer and borehole hydro-  
335 geophysical tests, again leading to systematic underestimation of groundwater velocities.

336 The four carbonate aquifers of Great Britain show a range of hydraulic behaviours that encompass those of karst  
337 aquifers worldwide and hence the presented findings are widely applicable to better predict contaminant transport in  
338 karst systems. For example, the underestimation of hydraulic conductivity by the use of pumping tests also occurs in  
339 intensively karstified aquifers of the Alpine regions of southern France, north-western Germany and central Italy.  
340 Comparison with studies of carbonate aquifers of northern America confirms the use of an excessive standard value  
341 (~5%) of effective porosity that is applied to contaminant transport models without support of tracer and hydro-  
342 geophysical tests, leading to further underestimation of groundwater velocities.

343 Overall, the findings of this review highlight how paucity or lack of large-scale pumping tests, tracer tests and site-  
344 scale hydro-geophysical testing leads to an underestimation of groundwater flow velocities up to two order of  
345 magnitude in both moderately or intensively karstified carbonate aquifer-types.

346

#### 347 **Acknowledgements**

348 The authors thank the research colleagues of the University of Leeds (UK) that contributed to advance knowledge of  
349 the UK karst aquifers over the years. Noelle Odling and Simon Bottrell are thanked for the interesting discussions on  
350 the four karst aquifers of Great Britain. Steven Banwart is thanked for funding recent published research that  
351 provided data for this review on the Magnesian Limestone aquifer. Neil Gunn (Atkins) and Daniele Coltellacci  
352 (Sapienza University of Rome) provided assistance on finding outcrop images and relevant papers, respectively.  
353 Critical discussions on the carbonate aquifers of Italy, France and Canada with Marco Petitta (Sapienza University  
354 of Rome), Hervé Jourde (Université de Montpellier) and Beth Parker (University of Guelph) were also appreciated.  
355 Nico Goldscheider (Karlsruhe Institute of Technology) has kindly provided the global map of karst aquifers. Finally,  
356 the manuscript benefitted from constructive review comments of two anonymous reviewers and Editor, Xianliang Yi  
357 (Nanjing University).

358

359 **References**

- 360 Abesser C, Lewis, M (2015) A semi-quantitative technique for mapping potential aquifer productivity on the  
361 national scale: example of England and Wales (UK). *Hydrogeol J* 23(8):1677-1694.
- 362 Agbotui PY, West LJ, Bottrell SH (2020) Characterisation of fractured carbonate aquifers using ambient borehole  
363 dilution tests. *J Hydrol* 589:125191.
- 364 Aliyu MM, Murphy W, Lawrence JA, Collier R (1997) Engineering geological characterization of flints. *Q J Eng*  
365 *Geol Hydrogeol* 50(2):133-147.
- 366 Allen DJ, Brewerton LJ, Coleby LM, Gibbs BR, Lewis MA, MacDonald AM, Wagstaff SJ, Williams AT (1997)  
367 The physical properties of major aquifers in England and Wales. BGS WD/97/34, British Geological Survey,  
368 Nottingham (UK)
- 369 Amoruso A, Crescentini L, Petitta M, Tallini M (2013) Parsimonious recharge/discharge modeling in carbonate  
370 fractured aquifers: the groundwater flow in the Gran Sasso aquifer (Central Italy). *J Hydrol* 476:136-146
- 371 Anderson MP, Cherry JA (1979) Using models to simulate the movement of contaminants through groundwater  
372 flow systems. *Crit Rev Environ Sci Technol* 9(2):97-156.
- 373 Assari A, Mohammadi Z (2017) Assessing flow paths in a karst aquifer based on multiple dye tracing tests using  
374 stochastic simulation and the MODFLOW-CFP code. *Hydrogeol J* 25(6):1679-1702.
- 375 Atkinson TC (1977) Diffuse flow and conduit flow in limestone terrain in the Mendip Hills, Somerset (Great  
376 Britain). *J Hydrol* 35(1-2):93-110.
- 377 Atkinson TC, Smart PL (1981) Artificial tracers in hydrogeology. In *A Survey of British Hydrogeology 1980*, 173–  
378 190. Royal Society, London (UK)
- 379 Berkowitz B (2002) Characterizing flow and transport in fractured geological media: A review. *Adv Water Resour*  
380 25(8-12):861-884
- 381 Berlin, M., Natarajan, N., Vasudevan, M., Kumar, G.S. (2020) Influence of transient porosity in a coupled fracture-  
382 skin-matrix system at the scale of a single fracture. *Environ Sci Pollut Resear* 1-19

- 383 Bird MJ, Allen DJ (1989) Hydraulic conductivity measurements of the Carboniferous Limestone, Mendip,  
384 Somerset. British Geological Survey Technical Report WD/89/57
- 385 Bloomfield J (1996) Characterisation of hydrogeologically significant fracture distributions in the Chalk: an  
386 example from the Upper Chalk of southern England. *J Hydrol* 184(3-4):355-379.
- 387 Bredehoeft J, King M (2010) Potential contaminant transport in the regional Carbonate Aquifer beneath Yucca  
388 Mountain, Nevada, USA. *Hydrogeol J* 18(3):775-789
- 389 Brunetti E, Jones JP, Petitta M, Rudolph DL (2013) Assessing the impact of large-scale dewatering on fault  
390 controlled aquifer systems: a case study in the Acque Albule basin (Tivoli, central Italy). *Hydrogeol J* 21:401-423.
- 391 Carey MA, Chadha D (1998) Modelling the hydraulic relationship between the River Derwent and the Corallian  
392 Limestone aquifer. *Q J Engineer Geol Hydrogeol* 31(1):63-72.
- 393 Chadwick RA (1993) Aspects of basin inversion in southern Britain. *J Geol Soc* 150(2):311-322.
- 394 Chen Z, Goldscheider N (2014) Modeling spatially and temporally varied hydraulic behavior of a folded karst  
395 system with dominant conduit drainage at catchment scale, Hochifien–Gottesacker, Alps. *J Hydrol* 514:41-52.
- 396 Cook SJ, Fitzpatrick CM, Burgess WG, Lytton L, Bishop P, Sage R (2012) Modelling the influence of solution-  
397 enhanced conduits on catchment-scale contaminant transport in the Hertfordshire Chalk aquifer. In: Shepley, M.G.,  
398 Whiteman, M.I., Hulme, P.J. and Grout M.W. (eds) *Groundwater Resources Modelling: A Case Study from the UK*.  
399 Geol Soc, London, Spec Publ 364(1):205-225.
- 400 Davison RM, Lerner DN (2000) Evaluating natural attenuation of groundwater pollution from a coal-carbonisation  
401 plant: developing a local-scale model using MODFLOW, MODTMR and MT3D. *Water Environ J* 14(6):419-426.
- 402 Doherty JE, Hunt RJ (2016) Approaches to highly parameterized inversion: a guide to using PEST for groundwater-  
403 model calibration. United States Geological Survey, 2010/5159
- 404 Downing RA, Smith DB, Pearson FJ, Monkhouse RA, Otlet RL (1977) The age of groundwater in the Lincolnshire  
405 Limestone, England and its relevance to the flow mechanism. *J Hydrol* 33(3-4):201-216.

- 406 Downing RA, Williams BJP (1969) The Groundwater Hydrology of the Lincolnshire Limestone. Water Resources  
407 Board, Reading, p. 160
- 408 Drew DP (2008) Hydrogeology of lowland karst in Ireland. *Q J Eng Geol Hydrogeol* 41(1):61-72.
- 409 Ducci, D., Della Morte, R., Mottola, A., Onorati, G., Pugliano, G. (2019) Nitrate trends in groundwater of the  
410 Campania region (southern Italy). *Environm Sci Pollut Resear* 26(3):2120-2131.
- 411 Ely DM, Burns ER, Morgan DS, Vaccaro JJ (2014) Numerical simulation of groundwater flow in the Columbia  
412 Plateau Regional Aquifer System, Idaho, Oregon, and Washington. United States Geological Survey, 2014-5127.
- 413 Environment Agency (2016) East Yorkshire Chalk Investigation: Numerical Modelling Update and recalibration.  
414 Report 62986 R2D1, Leeds (UK)
- 415 Environment Agency 2019. Manual for the production of Groundwater Source Protection Zones. Report 16864,  
416 Warrington (UK)
- 417 Farrant AR, Cooper AH (2008) Karst geohazards in the UK: the use of digital data for hazard management. *Quart J*  
418 *Eng Geol Hydrogeol* 41(3):339-356.
- 419 Foley A.E. (2006) The use and development of some groundwater tracers for wellhead protection: studies from the  
420 Corallian limestone of Yorkshire. PhD Thesis, University College, London, UK
- 421 Foley AE, Cachandt G, Franklin J, Willmore F, Atkinson T (2012) Tracer tests and the structure of permeability in  
422 the Corallian limestone aquifer of northern England, UK. *Hydrogeol J* 20(3):483-498.
- 423 Freeze AR, Cherry JA (1979) Groundwater. Prentice Hall, Upper Saddle Hall, NJ (USA)
- 424 Gallagher AJ, Rutter HK, Buckley DK, Molyneux I (2012) Lithostratigraphic controls on recharge to the Chalk  
425 aquifer of Southern England. *Quart J Engineer Geol Hydrogeol* 45(2):161-172.
- 426 Gallegos JJ, Hu BX, Davis H (2013) Simulating flow in karst aquifers at laboratory and sub-regional scales using  
427 MODFLOW-CFP. *Hydrogeol J* 21(8):1749-1760.

- 428 **Gárfias J, Llanos H, Martel R, Salas-García J, Bibiano-Cruz L (2018) Assessment of vulnerability and**  
429 **control measures to protect the Salbarua ecosystem from hypothetical spill sites. Environ Sci Pollut Res**  
430 **25(26):26228-26245.**
- 431 Gleeson T, Smith L, Moosdorf N, Hartmann J, Dürr HH, Manning AH, van Beek LP, Jellinek AM (2011) Mapping  
432 permeability over the surface of the Earth. *Geophys Resear Letters*, 38(2).
- 433 Goeppert N, Goldscheider N (2011) Transport and variability of fecal bacteria in carbonate conglomerate  
434 aquifers. *Groundwater* 49:77-84.
- 435 Golder Associates (2006) Guelph-Puslinch Groundwater Protection Study Ver. 4.0. Report 03-1112-016
- 436 Goldscheider N (2005) Karst groundwater vulnerability mapping: application of a new method in the Swabian Alb,  
437 Germany. *Hydrogeol J* 13(4):555-564
- 438 Goldscheider N, Drew D (2014) *Methods in Karst Hydrogeology: IAH: International Contributions to*  
439 *Hydrogeology*. Crc Press, Boca Raton, Florida (USA)
- 440 Goldscheider N, Chen Z, Auler A.S, Bakalowicz M, Broda S, Drew D, Hartmann J, Jiang G, Moosdorf N,  
441 Stevanovic Z, Veni G 2020. Global distribution of carbonate rocks and karst water resources. *Hydrogeology*  
442 *Journal* 28(5):1661-1677.
- 443 Gregory SP, Maurice LD, West JM, Goody DC (2014) Microbial communities in UK aquifers: current  
444 understanding and future research needs. *Q J Engineer Geol Hydrogeol* 47(2):145-157.
- 445 Hallam A (1971) Mesozoic geology and the opening of the North Atlantic. *J Geol* 79(2):129-157.
- 446 Hancock JM (1975) The petrology of the Chalk. *Proc Geol Assoc* 86(4):499-535.
- 447 Hartmann A, Goldscheider N, Wagener T., Lange, J Weiler M (2014) Karst water resources in a changing world:  
448 Review of hydrological modeling approaches. *Rev Geophys* 52(3):218-242.
- 449 Hartmann S, Odling NE, West LJ (2007) A multi-directional tracer test in the fractured Chalk aquifer of E.  
450 Yorkshire, UK. *J Contam Hydrol* 94(3-4):315-331.

- 451 Hill ME, Stewart MT, Martin A (2010) Evaluation of the MODFLOW-2005 conduit flow  
452 process. *Groundwater* 48(4):549-559.
- 453 Hobbs SL (1988) Recharge, flow and storage in the unsaturated zone of the Mendip limestone aquifer. PhD Thesis,  
454 Bristol University
- 455 Hobbs SL, Gunn J (1998) The hydrogeological effect of quarrying karstified limestone: options for prediction and  
456 mitigation. *Q J Eng Geol Hydrogeol* 31(2):147-157.
- 457 Hu Y, Xu W, Zhan L, Li J, Chen Y (2020) Quantitative characterization of solute transport in fractures with  
458 different surface roughness based on ten Barton profiles. *Environ Sci Pollut Resear* 1-16.
- 459 Hussein ME, Odling NE, Clark RA (2013) Borehole water level response to barometric pressure as an indicator of  
460 aquifer vulnerability. *Water Resour Resear* 49(10):7102-7119.
- 461 Jeans CV (1980) Early submarine lithification in the Red Chalk and Lower Chalk of eastern England: a bacterial  
462 control model and its implications. *Proceed York Geol Soc* 43(2):81-157.
- 463 **John DE, Rose JB (2005) Review of factors affecting microbial survival in groundwater. *Environ Sci***  
464 ***Technol* 39(19):7345-7356**
- 465 Johnson CR, Greenkorn RA, Woods EG (1966) Pulse-testing: a new method for describing reservoir flow properties  
466 between wells. *J Petrol Technol* 18(12):1-599.
- 467 Jones BR, Brouwers LB, Van Tonder WD, Dippenaar MA (2017) Assessing geotechnical centrifuge modelling in  
468 addressing variably saturated flow in soil and fractured rock. *Environ Sci Pollut Resear* 24(15):3203-3223.
- 469 Kana AA, West LJ, Clark RA (2013) Fracture aperture and fill characterization in a limestone quarry using GPR  
470 thin-layer AVA analysis. *Near Surf Geophys* 11(3):293-306.
- 471 **Király L (1975) Rapport sur l'état actuel des connaissances dans le domaine des caractères physiques des**  
472 **roches karstiques. *Hydrogeology of karstic terrains (Hydrogéologie des terrains karstiques)*. Internat Union**  
473 ***Geol Sci* 3:53-67**

- 474 Le Borgne T, Bour O, Paillet FL, Caudal JP (2006) Assessment of preferential flow path connectivity and hydraulic  
475 properties at single-borehole and cross-borehole scales in a fractured aquifer. *J Hydrol* 328(1-2):347-359.
- 476 Little R, Muller E, Mackay R (1996) Modelling of contaminant migration in a chalk aquifer. *J Hydrol* 175(1-4):473-  
477 509
- 478 Liu F, Yi S, Ma H, Huang J, Tang Y, Qin J, Zhou WH (2019) Risk assessment of groundwater environmental  
479 contamination: a case study of a karst site for the construction of a fossil power plant. *Environ Sci Pollut*  
480 *Resear* 26(30):30561-30574.
- 481 MacDonald AM, Allen DJ (2001) Aquifer properties of the Chalk of England. *Q J Eng Geol Hydrogeol* 34(4):371-  
482 384.
- 483 Maldaner CH, Quinn PM, Cherry JA, Parker BL (2018) Improving estimates of groundwater velocity in a fractured  
484 rock borehole using hydraulic and tracer dilution methods. *J Contam Hydrol* 214:75-86
- 485 Maurice LD, Atkinson TC, Barker JA, Bloomfield JP, Farrant AR, Williams AT (2006) Karstic behaviour of  
486 groundwater in the English Chalk. *J Hydrol* 330(1-2):63-70.
- 487 Mawson M, Tucker M (2009) High-frequency cyclicity (Milankovitch and millennial-scale) in slope-apron  
488 carbonates: Zechstein (Upper Permian), North-east England. *Sedimentology* 56(6):1905-1936.
- 489 Medici G, West LJ, Mounney NP (2016) Characterizing flow pathways in a sandstone aquifer: tectonic vs  
490 sedimentary heterogeneities. *Journal of Contaminant Hydrology* 194:36-58
- 491 Medici G, West LJ, Banwart SA (2019a) Groundwater flow velocities in a fractured carbonate aquifer-type:  
492 Implications for contaminant transport. *J Contam Hydrol* 222:1-16
- 493 Medici G, West LJ, Chapman PJ, Banwart SA (2019b) Prediction of contaminant transport in fractured carbonate  
494 aquifer-types; case study of the Permian Magnesian Limestone Group (NE England, UK) *Environ Sci Pollut Resear*  
495 26:24863-24884

- 496 Medici G, West LJ, Mountney NP, Welch M (2019c) Permeability of rock discontinuities and faults in the Triassic  
497 Sherwood Sandstone Group (UK): insights for management of fluvio-aeolian aquifers worldwide. *Hydrogeol*  
498 *J* 27(8):2835-2855.
- 499 Medici G, Baják P, West LJ, Chapman PJ, Banwart SA (2021a) DOC and nitrate fluxes from farmland; impact on a  
500 dolostone aquifer KCZ. *J Hydrol* 595:125658
- 501 Medici G, Smeraglia L, Torabi A, Botter C (2021b) A Review of Modelling Approaches to Deformed Carbonate  
502 Aquifers. *Groundwater* 59(3):334-351
- 503 Neymeyer A, Williams RT, Younger PL (2007) Migration of polluted mine water in a public supply aquifer. *Q J*  
504 *Eng Geol Hydrogeol* 40(1):75-84
- 505 Noushabadi MJ, Jourde H, Massonnat G (2011) Influence of the observation scale on permeability estimation at  
506 local and regional scales through well tests in a fractured and karstic aquifer (Lez aquifer, Southern France). *J*  
507 *Hydrol* 103:321-336
- 508 Odling NE, West LJ, Hartmann S, Kilpatrick A (2013) Fractional flow in fractured chalk; a flow and tracer test  
509 revisited. *J Contam Hydrol* 147:96-111.
- 510 Palmucci W, Rusi S, Di Curzio D (2016) Mobilisation processes responsible for iron and manganese contamination  
511 of groundwater in Central Adriatic Italy. *Environ Sci Pollut Resear* 23(12):11790-805.
- 512 Parker BL, Bairos K, Maldaner CH, Chapman SW, Turner CM, Burns LS, Plett J, Carter R, Cherry JA (2019)  
513 Metolachlor dense non-aqueous phase liquid source conditions and plume attenuation in a dolostone water supply  
514 aquifer. In: Ofterdinger, U., MacDonald, A.M., Compte J.C. and Young M.E. (eds) *Groundwater in Fractured*  
515 *Bedrock Environments: Managing Catchment and Subsurface Resources*. Geol Soc, London, Spec Publ 479(1):207-  
516 236.
- 517 Perrin J, Parker BL, Cherry JA (2011) Assessing the flow regime in a contaminated fractured and karstic dolostone  
518 aquifer supplying municipal water. *J Hydrol* 400(3-4):396-410.

- 519 Pringle JK, Westerman AR, Schmidt A, Harrison J, Shandley D, Beck J, Donahue RE, Gardiner AR (2002)  
520 Investigating Peak Cavern, Castleton, Derbyshire, UK: Integrating cave survey, geophysics, geology and  
521 archaeology to create a 3D digital CAD model. *Cave Karst Sci* 29(2):67-74.
- 522 Quinn PM, Cherry JA, Parker BL (2011) Quantification of non-Darcian flow observed during packer testing in  
523 fractured sedimentary rock. *Water Resour Resear* 47(9).
- 524 Quinn PM, Parker BL, Cherry JA (2011) Using constant head step tests to determine hydraulic apertures in fractured  
525 rock. *J Contam Hydrol* 126(1-2):85-99
- 526 Reh, R., Licha, T., Nödler, K., Geyer, T., Sauter, M. (2015) Evaluation and application of organic micro-pollutants  
527 (OMPs) as indicators in karst system characterization. *Environ Sci Pollut Resear* 22(6):4631-4643.
- 528 Ren S, Gragg S, Zhang Y, Carr BJ, Yao G (2018) Borehole characterization of hydraulic properties and groundwater  
529 flow in a crystalline fractured aquifer of a headwater mountain watershed, Laramie Range, Wyoming. *J Hydrol* 561:  
530 780-795
- 531 Ren, K., Pan, X., Zeng, J., Yuan, D. (2019) Contaminant sources and processes affecting spring water quality in a  
532 typical karst basin (Hongjiadu Basin, SW China): insights provided by hydrochemical and isotopic data. *Environ Sci*  
533 *Pollut Resear* 26(30):31354-31367.
- 534 Reimann T, Hill ME (2009) MODFLOW-CFP: A new conduit flow process for MODFLOW–  
535 2005. *Groundwater* 47(3):321-325.
- 536 Rivett MO, Smith JWN, Buss SR, Morgan P (2007) Nitrate occurrence and attenuation in the major aquifers of  
537 England and Wales. *Q J Engin Geol Hydrogeol* 40(4):335-352.
- 538 Romm, E.S. 1966. Flow characteristics of fractured rocks. Nedra, Moscow (Russia)
- 539 Rusi S, Di Curzio D, Palmucci W, Petaccia R (2018) Detection of the natural origin hydrocarbon contamination in  
540 carbonate aquifers (central Apennine, Italy). *Environ Sci Pollut Res* 25(16):15577-15596.
- 541 Saller SP, Ronayne MJ, Long AJ (2013) Comparison of a karst groundwater model with and without discrete  
542 conduit flow. *Hydrogeol J* 21(7):1555-1566.

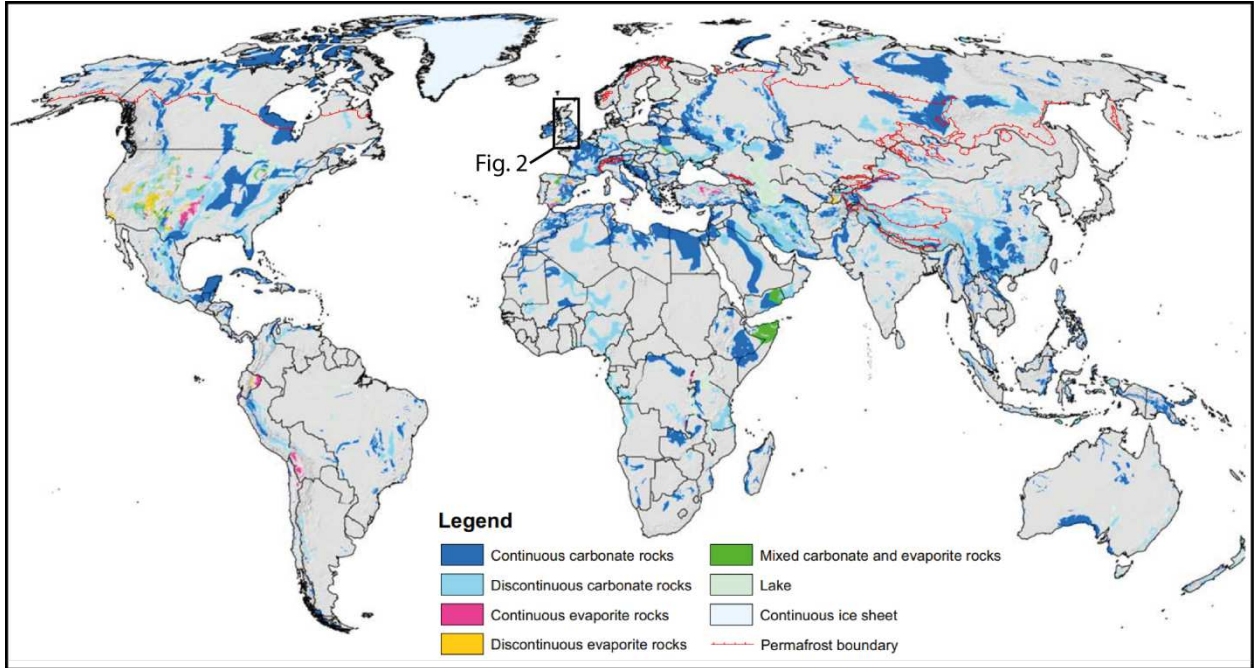
- 543 Sauter M (1992) Quantification and forecasting of regional groundwater flow and transport in a karst aquifer  
544 (Gallusquelle, Malm, SW. Germany). *Tübinger Geowiss Arb*, C13. [http://tobias-lib.uni-](http://tobias-lib.uni-tuebingen.de/volltexte/2005/2039/pdf/13.pdf)  
545 [tuebingen.de/volltexte/2005/2039/pdf/13.pdf](http://tobias-lib.uni-tuebingen.de/volltexte/2005/2039/pdf/13.pdf)
- 546 Schulze-Makuch D, Carlson DA, Cherkauer DS, Malik P (1999) Scale dependency of hydraulic conductivity in  
547 heterogeneous media. *Groundwater* 37(6):904-919.
- 548 Shepley MG, Whiteman MI, Hulme PJ, Grout MW (2012) Introduction: groundwater resources modelling: a case  
549 study from the UK. Geological Society, London, Special Publications, 364(1):1-6.
- 550 Sorensen JP, Maurice L, Edwards FK, Lapworth DJ, Read DS, Allen D, Butcher AS, Newbold LK, Townsend BR,  
551 Williams PJ (2013) Using boreholes as windows into groundwater ecosystems. *PLoS One* 8(7):70264.
- 552 Souque C, Knipe RJ, Davies RK, Jones P, Welch MJ, Lorenz J (2019) Fracture corridors and fault reactivation:  
553 Example from the Chalk, Isle of Thanet, Kent, England. *J Struct Geol* 122:11-26.
- 554 Sullivan TP, Gao Y, Reimann T (2019) Nitrate transport in a karst aquifer: Numerical model development and  
555 source evaluation. *J Hydrol* 573:432-448.
- 556 Taylor R, Cronin A, Pedley S, Barker J, Atkinson T (2004) The implications of groundwater velocity variations on  
557 microbial transport and wellhead protection—review of field evidence. *FEMS Microbiol Ecol* 49:17-26.
- 558 Tranter J, Gunn J, Hunter C, Perkins J (1997) Bacteria in the castleton karst, derbyshire, England. *Q J Eng Geol*  
559 *Hydrogeol* 30(2):171-178.
- 560 Tucker ME (1991) Sequence stratigraphy of carbonate-evaporite basins: models and application to the Upper  
561 Permian (Zechstein) of northeast England and adjoining North Sea. *J Geol Soc* 148(6):1019-1036.
- 562 Wealthall GA, Thornton SF, Lerner DN (2001) Assessing the transport and fate of MTBE-amended petroleum  
563 hydrocarbons in the chalk aquifer, UK. In: Thornton, S.F., Oswald, S.E. (Eds.), *Groundwater quality: Natural*  
564 *attenuation of groundwater pollution*. IAHS Publication, 275:205–211

- 565 Wang L, Stuart ME, Bloomfield JP, Butcher AS, Goody DC, McKenzie AA, Lewis MA, Williams A (2012)  
566 Prediction of the arrival of peak nitrate concentrations at the water table at the regional scale in Great  
567 Britain. *Hydrol Process* 26(2):226-239.
- 568 West LJ, Odling NE (2007) Characterization of a multilayer aquifer using open well dilution  
569 tests. *Groundwater* 45(1):74-84.
- 570 Wignall PB, Newton R (2001) Black shales on the basin margin: a model based on examples from the Upper  
571 Jurassic of the Boulonnais, northern France. *Sediment Geol* 144(3-4):335-356.
- 572 White WB (2002) Karst hydrology: recent developments and open questions. *Engineer Geol* 65(2-3):85-105.
- 573 Worthington SRH (2015) Diagnostic tests for conceptualizing transport in bedrock aquifers. *J Hydrol* 529:365-372.
- 574 Worthington SRH, Ford DC (2009) Self-organized permeability in carbonate aquifers. *Groundwater* 47(3):326-336.
- 575 Worthington SR, Smart CC, Ruland W (2012) Effective porosity of a carbonate aquifer with bacterial  
576 contamination: Walkerton, Ontario, Canada. *J Hydrol* 464:517-527
- 577 Yager RM, Plummer LN, Kauffman LJ, Doctor DH, Nelms DL, Schlosser P (2013) Comparison of age distributions  
578 estimated from environmental tracers by using binary-dilution and numerical models of fractured and folded karst:  
579 Shenandoah Valley of Virginia and West Virginia, USA. *Hydrogeol J* 21(6):1193-1217
- 580 Zuffianò LE, Basso A, Casarano D, Dragone V, Limoni PP, Romanazzi A, Santaloia F, Polemio M (2016) Coastal  
581 hydrogeological system of mar Piccolo (Taranto, Italy). *Environ Sci Pollut Resear* 23(13):12502-12514.
- 582 Zwahlen F (2003) Vulnerability and risk mapping for the protection of carbonate (karst) aquifers. Office for Official  
583 Publications of the European Communities, Bruxelles (Belgium).
- 584
- 585
- 586
- 587

588 **Figures**

589

590

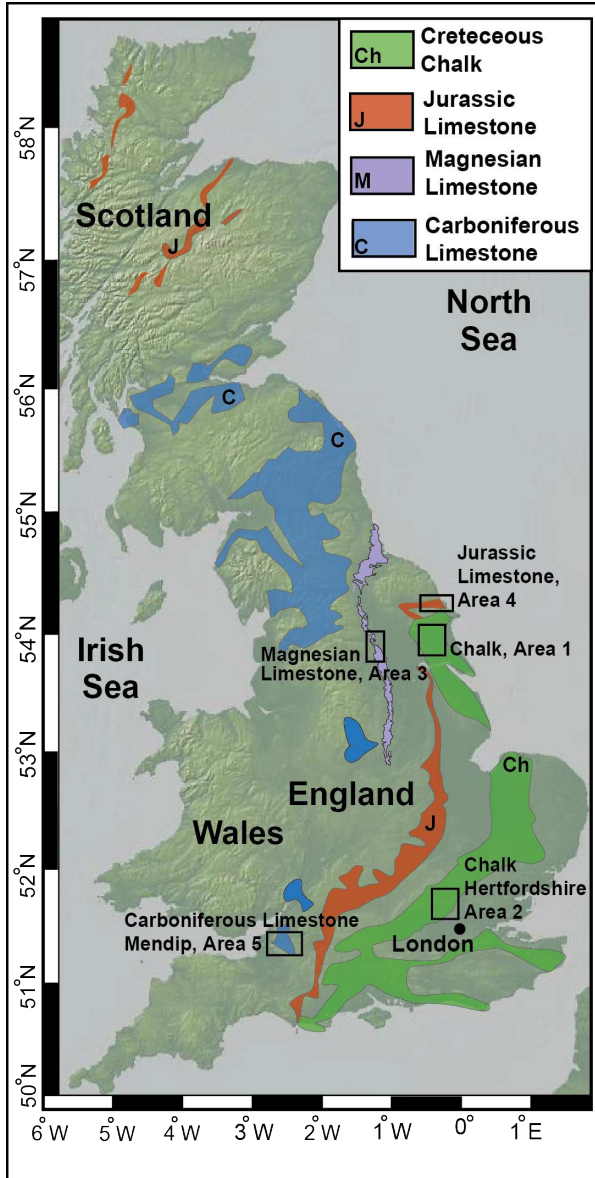


591

592 **Fig. 1** Worldwide distribution of karst aquifers of carbonate, evaporate and ice sheet origin (from Goldscheider et al.

593 2020)

594



595

596 **Fig. 2** Outcrop patterns of four karst aquifer of Great Britain (from Allen et al. 1997) and location of the study areas

597 referred to in the text

598

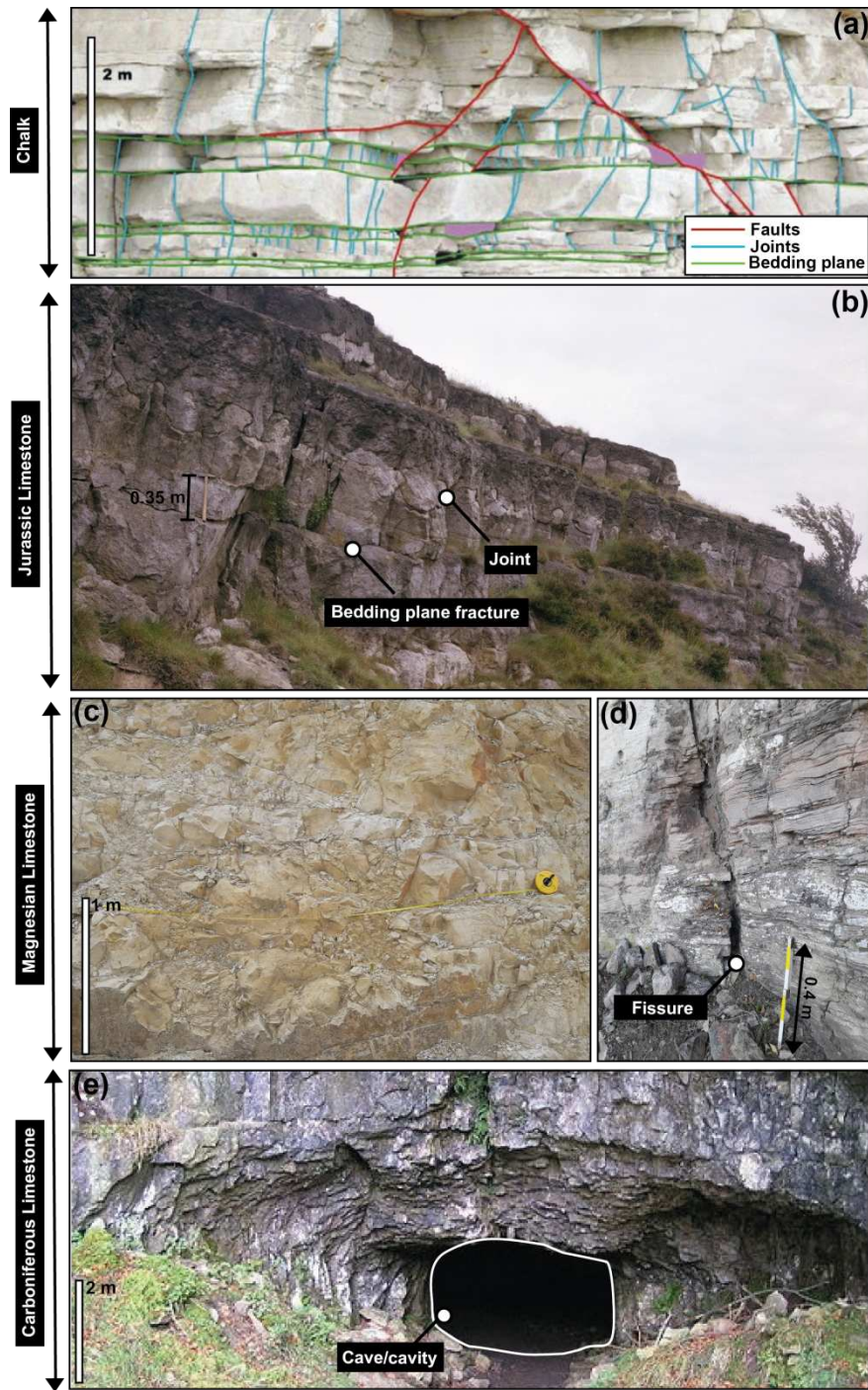
599

600

601

602

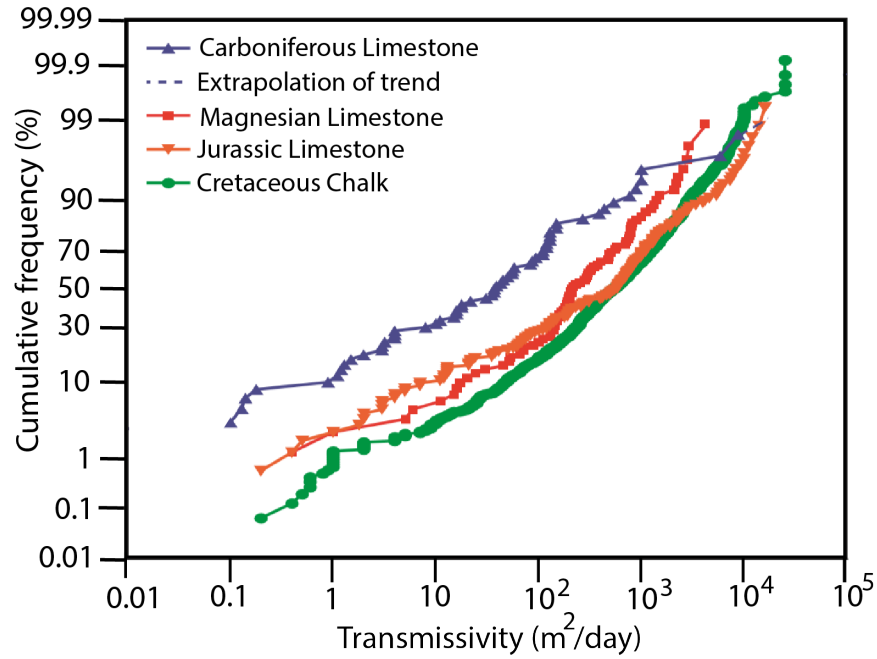
603



604

605 **Fig. 3** Carbonate aquifers of Great Britain in outcrop: **a** The Northern Province Chalk at Flamborough Head, NE606 Yorkshire (from Hartman et al. 2007), **b** The Jurassic Limestone at Whitestone Scar, Thornton, NE Yorkshire, **c**607 Fracturing pattern in the Magnesian Limestone at the Wellhouse Farm Quarry, Tadcaster, Yorkshire, **d** Detail of608 karstic fissure in the Magnesian Limestone at the Byram Nurseries Quarry, Leeds, Yorkshire, **e** The Yordas Cave at

609 Kingsdale, North Yorkshire

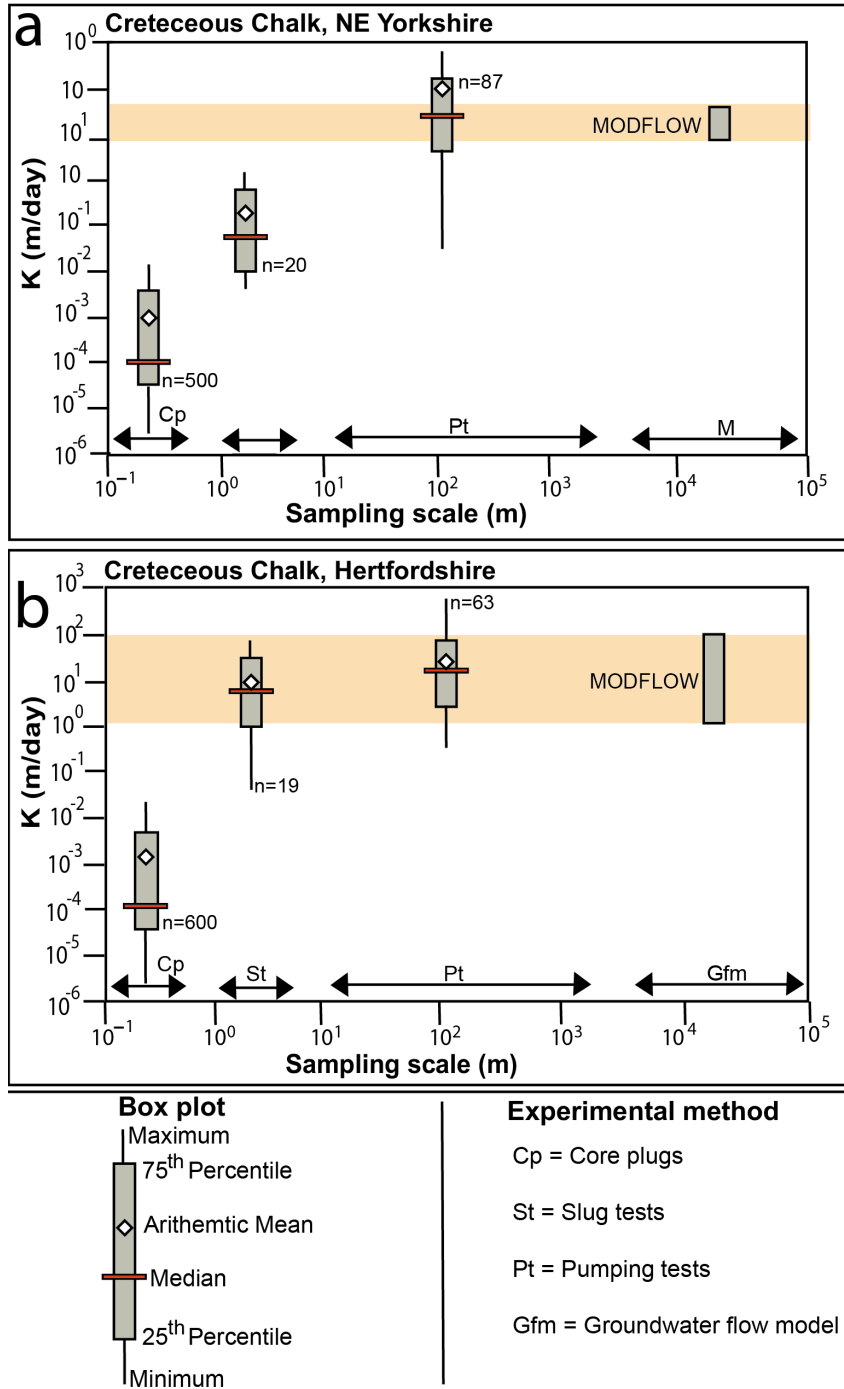


610

611 **Fig. 4** Cumulative frequency of transmissivity from pumping tests in the Chalk, Jurassic Limestone, Magnesian

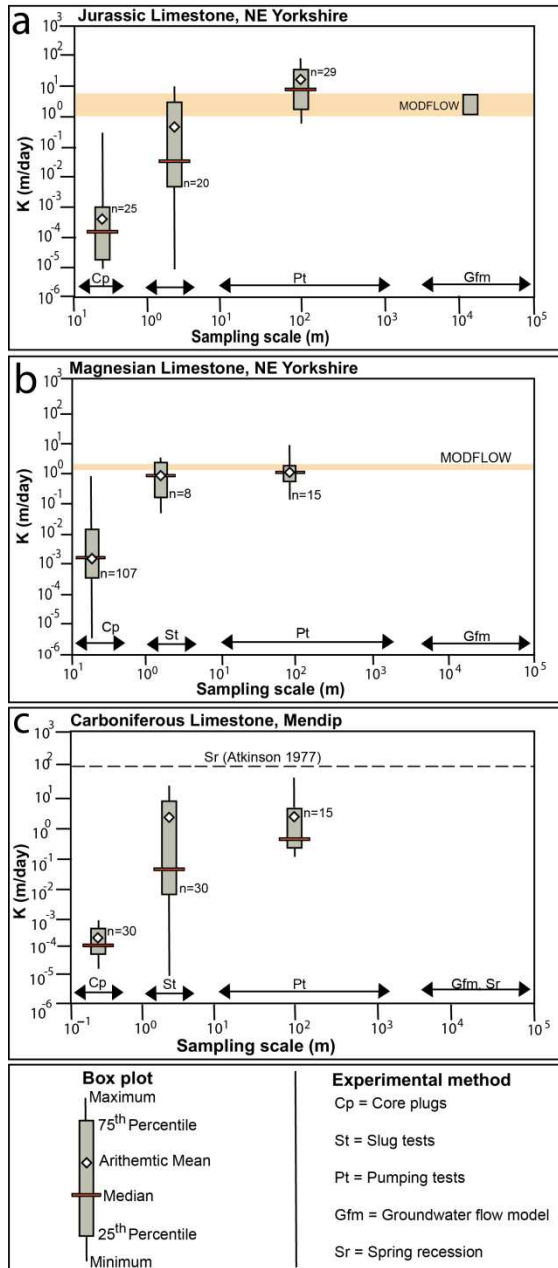
612 Limestone and Carboniferous Limestone aquifers of Great Britain (from Worthington and Ford 2009).

613



614

615 **Fig. 5** Hydraulic conductivity vs. scale: **a** Chalk aquifer, Northern Province (NE Yorkshire) with data from core-  
 616 plug (Allen et al. 1997), slug (Hussein et al. 2013), pumping (Allen et al. 1997) tests and a MODFLOW numerical  
 617 model (Environment Agency 2016), **b** Southern Province (Hertfordshire) with data from core-plug (Allen et al.  
 618 1997), slug (Wealthall et al. 2001), pumping tests (Allen et al. 1997) and a MODFLOW numerical model (Cook et  
 619 al. 2012).



620

621 **Fig. 6** Hydraulic conductivity vs. scale: **a** Jurassic Limestone aquifer of NE Yorkshire with data from core-plug

622 (Allen et al. 1997), slug (Allen et al. 1997), pumping tests (Allen et al. 1997) and a MODFLOW numerical model

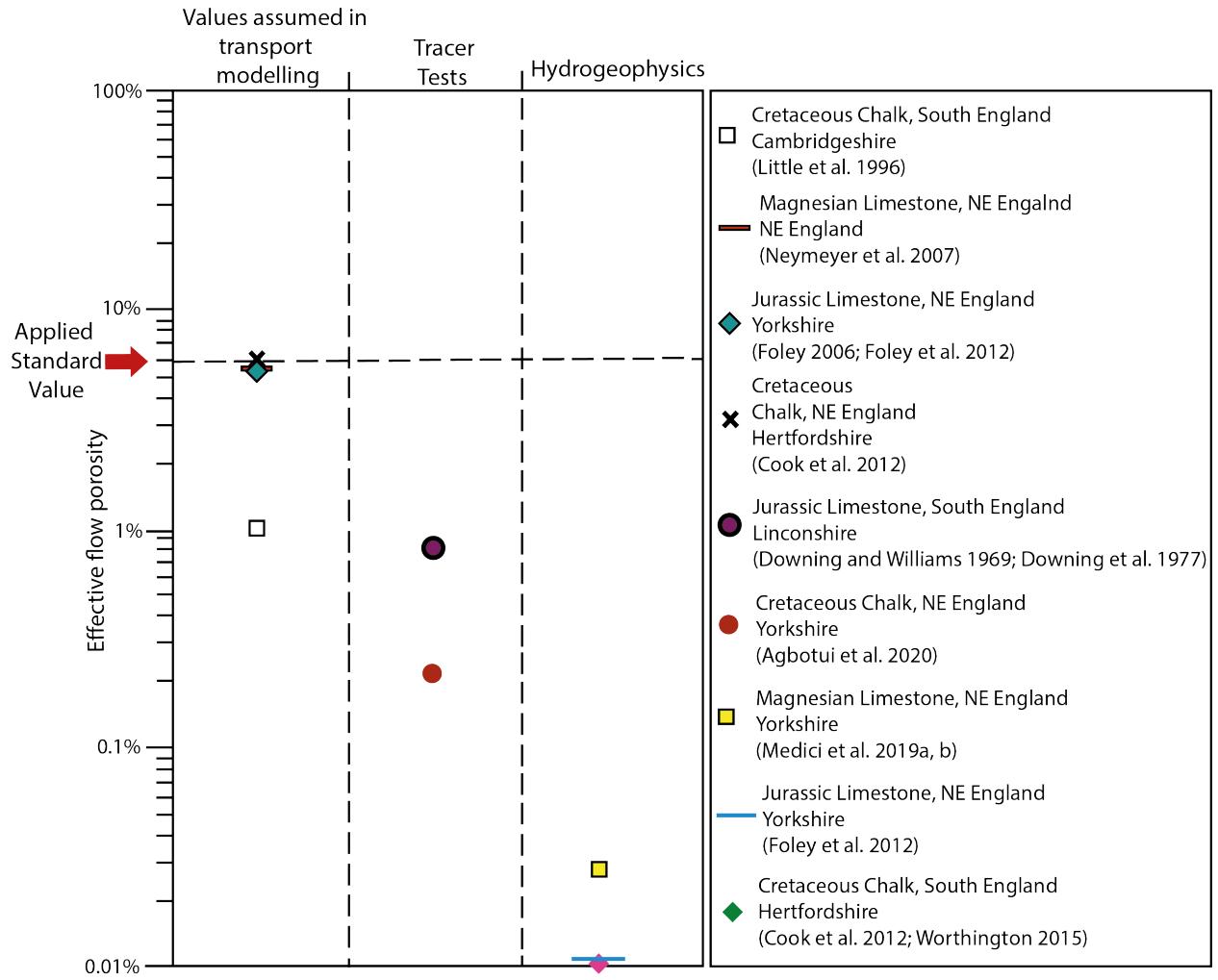
623 (Carey and Chadha 1998), **b** Magnesian Limestone aquifer of NE Yorkshire with data from core-plug (Allen et al.

624 1997), slug (Medici et al. 2019a), pumping tests (Allen et al. 1997) and a MODFLOW numerical model (Medici et

625 al. 2019b), **c** Carboniferous Limestone aquifer of the Mendips in Somerset, southern England with data from core-

626 plug (Allen et al. 1997), slug (Hobbs 1988), pumping tests (Bird and Allen 1989) and from analysis of data from

627 spring recession (Atkinson 1977).



628

629 **Fig. 7** Effective porosity in the Chalk, Jurassic Limestone, Magnesian Limestone and Carboniferous Limestone  
 630 aquifers of Great Britain from hydrogeophysical characterisation (right panel) versus values assumed in previous  
 631 solute transport modelling studies (left panel).

632

633 **Declarations**

634

635 Ethics approval and consent to participate

636 Note applicable

637

638 Consent for publication

639 Note applicable

640

641 Availability of data and materials

642 The data that supports the findings of this study are available from the corresponding author upon reasonable request

643

644 Competing interests

645 The authors declare that they have no competing interests

646

647 Funding

648 Not applicable

649

650 Authors contribution

651 Giacomo Medici: Conceptualization, Data curation, Writing; Jared West: Supervision, Conceptualization

652

653